International Journal of Nephrology and Renovascular Disease

Dovepress

open access to scientific and medical research

Open Access Full Text Article

ORIGINAL RESEARCH

Serial changes in vessel walls of renal arteries after catheter-based renal artery denervation: insights from volumetric computed tomography analysis

This article was published in the following Dove Press journal:
International Journal of Nephrology and Renovascular Disease

Yu Kataoka[1]
Sinny Delacroix[2]
Samuel Sidharta[2]
Jordan Andrews[1]
Stephen J Nicholls[1]
Costas P Tsioufis[3]
Vasilios Papademetriou[4]
Stephen G Worthley[2]

[1]Vascular Research Center, South Australian Health and Medical Research Institute, University of Adelaide, Adelaide, SA, Australia; [2]Department of Medicine, Cardiovascular Research Center, Royal Adelaide Hospital, University of Adelaide, Adelaide, SA, Australia; [3]1st Department of Cardiology, University of Athens, Hippokration Hospital, Athens, Greece; [4]Center for hypertension, kidney and vascular research, VA and Georgetown University Medical Centers, Washington DC, USA

Aim: Radiofrequency ablation of peri-arterial renal autonomic nerves has been studied as a potential therapeutic option for resistant hypertension. While recent clinical trials have reported its efficacy, there is paucity of data addressing the effects of the procedure on renal arteries, such as changes in vessel and lumen areas. Herein, the effect of atheroma burden on renal arteries after renal denervation was assessed using computed tomography (CT) imaging.

Materials and methods: Serial renal artery CT imaging was conducted in 38 patients from the EnligHTN™ I study, a prospective, multicenter study evaluating the efficacy of the EnligHTN multi-electrode radiofrequency ablation catheter in resistant hypertensive subjects. Cross-sectional images of renal arteries at 1 mm intervals were acquired using commercially available software (3mensio Structural Heart version 5.1). Vessel and lumen areas were manually traced in each image. Vessel wall volume (VWV) and percent vessel wall volume (P-VWV) were calculated. The measurements within the ablation (first 30 mm segments) and the non-ablation (subsequent 30 mm segment after the first bifurcation of renal arteries) zones were compared.

Results: On serial evaluation, greater increase in P-VWV and VWV was observed in the ablation zone (change in P-VWV, 6.7%±5.1% vs 3.6%±2.8%, P=0.001; change in VWV, 106.3±87.4 vs 23.0±18.2 mm^3, P=0.001). Receiver-operating characteristic analysis demonstrated baseline P-VWV in the ablation zone >37.1% as an optimal cutoff value to predict its substantial progression after the procedure (area under the curve=0.88, sensitivity 89.8%, specificity 79.1%).

Conclusion: Change in vessel wall was greater within the segments receiving renal artery denervation. Baseline VWV predicted its substantial increase after the procedure. These observations suggest that atheroma burden within the renal arteries is a potential contributing factor to vascular changes after renal sympathetic denervation.

Keywords: renal artery, blood pressure, resistant hypertension, renal denervation, computed tomography

Correspondence: Sinny Delacroix
Cardiovascular Research Center, Royal Adelaide Hospital and Department of Medicine, University of Adelaide, Cardiovascular Investigation Unit, Port Road, Adelaide, SA 5000, Australia
Tel +61 8 7074 1776
Fax +61 8 7074 6182
Email sinny.delacroix@adelaide.edu.au

Introduction

Percutaneous catheter-based radiofrequency ablation has been a relatively recent development in the field of renal sympathetic denervation.[1–3] Early trials such as Symplicity-HTN 1, 2 and registry data[4–6] showed significant decreases in blood pressures in patients with resistant hypertension, but the only randomized, sham-controlled Symplicity-HTN 3 trial failed to mirror the same.[7] The safety of this procedure, nevertheless, has been established across the Symplicity-HTN 3 trial and other clinical trials.[4–8] However, there

submit your manuscript | www.dovepress.com
Dovepress
http://dx.doi.org/10.2147/IJNRD.S161313

are several observations suggesting the potential risk of renal artery stenosis after radiofrequency ablation. A preclinical study using a porcine model has shown that renal sympathetic denervation induced fibrous tissue development and strong inflammatory infiltration with vasculogenesis.[9] In addition, there are case reports showing the occurrence of renal artery stenosis in patients who received the procedure.[10–12] These observations may suggest that renal sympathetic denervation has the potential to cause renal artery stenosis in an artery with increased atheroma burden, emphasizing the need for renal artery imaging and assessment prior to procedure.

The EnligHTN™ I trial was a prospective, multicenter, non-randomized study to evaluate the clinical efficacy and safety of the EnligHTN multi-electrode radiofrequency ablation catheter in patients with resistant hypertension.[13] Since preoperative and 6-month follow-up computed tomography (CT) imaging of renal arteries were conducted in most of the subjects, we sought to analyze serial changes in the vessel wall of renal arteries after renal sympathetic denervation.

Materials and methods

EnligHTN I trial protocol

The details of the EnligHTN I trial have been described in detail previously.[13] In brief, 46 patients with drug-resistant hypertension were enrolled to assess the efficacy and safety of the EnligHTN multi-electrode system. Drug-resistant hypertension was defined as office systolic blood pressure ≥160 mmHg (≥150 mmHg for patients with type 2 diabetes), despite the stable use of ≥3 antihypertensive medications concurrently at maximally tolerated doses.

The renal denervation procedure was performed as previously described using the St Jude EnligHTN renal denervation system (St Jude Medical, St Paul, MN, USA).[13] Briefly, the ablation catheter consists of an expandable electrode basket with four platinum–iridium (Pt–Ir) ablation electrodes. The catheter was placed at the proximal to the first bifurcation of renal arteries using an 8F guiding catheter under fluoroscopy. Renal artery denervation was commenced and performed sequentially for both renal arteries by all four electrodes. After the first ablation, the catheter was repositioned proximally to avoid overlap of ablation segments and the ablation was repeated.

CT data acquisition

In the EnligHTN I study, serial renal artery CT imaging was conducted before the procedure and at the 6-month follow-up visit in the study subjects. Since baseline and follow-up CT were not undertaken in 5 and 3 patients, respectively, the remaining 38 patients who had evaluable paired renal artery CT imaging data were analyzed in the current study. A plain and contrast-enhanced CT was performed as described previously.[13]

Measurements of atheroma burden within renal arteries by CT imaging

The off-line analysis of acquired CT images was separately accomplished with commercially available software (3mensio Structural Heart version 7.0) as reported previously.[14] First, from the three multiplanar reformation planes and the three-dimensional reconstruction, the renal artery was automatically segmented and a centerline across the lumen was displayed. The centerline was manually adjusted and positioned to obtain the most accurate measurements. After validation of the centerline, the software automatically displays the short-axis view of the renal artery. Window settings were optimized to best differentiate the lumen from the vessel wall. Subsequent measurements were performed in double-oblique cross-sectional images after multiplanar reconstruction along the centerline.

Manual planimetry was used to trace the leading edges of the luminal and outer wall boundaries at 1 mm interval from the ostium to the distal end of renal arteries. The plaque area was defined as the difference in area occupied by the lumen (lumen area) and the outer wall boundaries (vessel area), as shown in Figure 1. As guiding catheter placement might cause injury of vessel wall, potentially leading to atheroma progression, we excluded the first 5 mm segment of renal arteries from the measurement of atheroma burden.

In the EnligHTN I trial, renal ablation was performed at the proximal segment to the first bifurcation of renal arteries. Based on this procedural characteristic, the "ablation zone" was defined as the segment between 5 mm distal to the ostium and the first bifurcation. Within the ablation zone, the vessel wall volume (VWV) was calculated by the summation of plaque area in each measured image. This value was then normalized to account for differences in the length of "ablation zone" between each subject by using the averaged length of ablation zone as follows:

$$\text{VWV } (\text{mm}^3) = [\Sigma(\text{vessel area} - \text{lumen area})/\text{number of slices in the ablation zone}] \times \text{averaged length of the ablation zone}$$

The percent VWV (P-VWV) was defined as the proportion of entire VWV occupied by atheroma burden within the ablation zone:

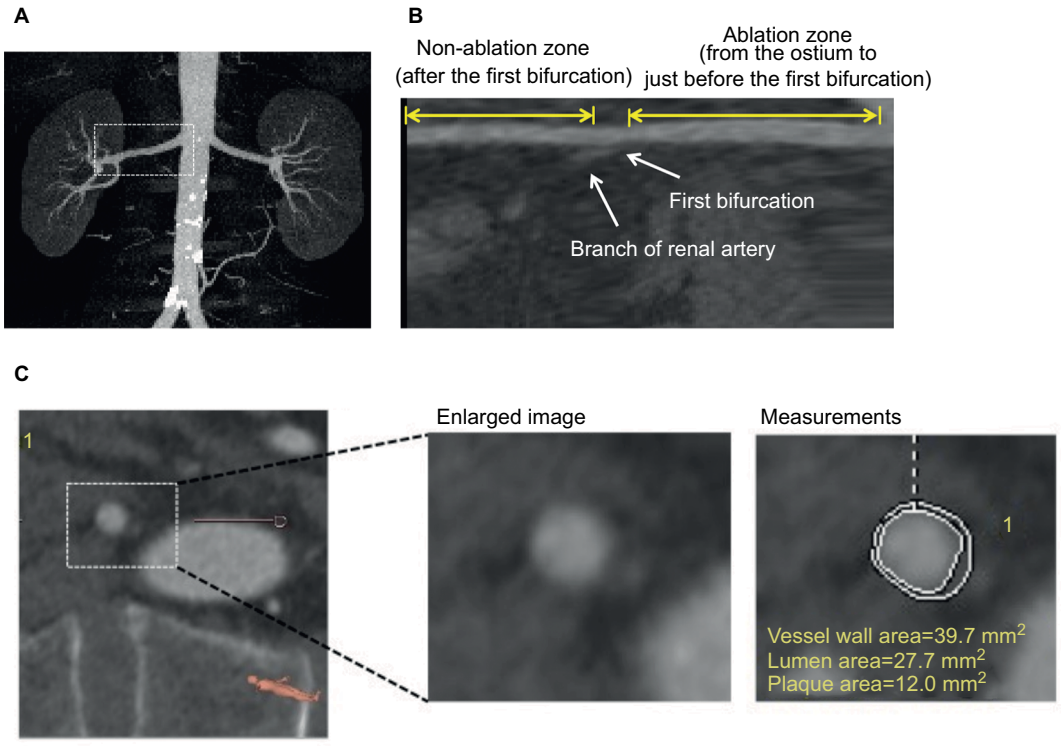

Figure 1 Volumetric CT analysis of vessel wall in renal arteries.
Notes: Cross-sectional images at 1 mm interval were created in the ablation and non-ablation zones. Lumen and outer wall boundaries were traced in all the slices. (**A**) MIP image of entire renal arteries and aorta. (**B**) Longitudinal view of the renal artery. (**C**) Cross-sectional image and measurement of the vessel and lumen areas.
Abbreviations: CT, computed tomography; MIP, maximum intensity projection.

P-VWV (%)=[Σ(vessel area − lumen area)/Σvessel area]×100

Non-ablation zone was defined as the segment after the first bifurcation. The length of the non-ablation zone was the same as the ablation zone in each subject. VWV within the "non-ablation zone" was calculated and then normalized using the above formula and P-VWV was also measured as described above.

Volumes occupied by the lumen and outer wall boundaries were similarly calculated by summation of their respective areas in each measured image. These analyses and measurements were conducted in both renal arteries.

Statistical analysis

Continuous variables are expressed as mean ± SD or median and categorical variables as percentages. Continuous data were compared using unpaired *t*-tests, or with Mann–Whitney log-rank tests when the variable was not normally distributed. To test the ability of CT-derived percent atheroma volume to predict substantial plaque progression, receiver-operating characteristic analyses and calculations of sensitivity, specificity, and positive and negative predictive values were performed. A value of $P<0.05$ was considered significant. All statistical analyses were performed using JMP software version 11.0.1 (SAS Institute, Cary, NC, USA).

Ethics approval and consent to participate

The Royal Adelaide Hospital ethics committee approved the study and all patients provided written informed consent. The EnligHTN I trial is registered with Clinical Trials Registry (NCT01438229).

Results

Patients' characteristics

The clinical characteristics are summarized in Table 1. Study subjects were on average 60 years old with a mean body mass index >30 kg/m^2 and were predominantly Caucasian. Type 2 diabetes mellitus and dyslipidemia were observed in 35.0% and 62.5% of the study subjects, respectively (Table 1) and 60% of these patients were on statin treatment for dyslipidemia.

Baseline CT measures

Seventy-six renal arteries in 38 resistant hypertensive patients were analyzed at baseline and 6-month follow-up.

Table 1 Baseline characteristics

Variables (n=38)	
Age (years)	60.8±10.3
Male, n (%)	27 (71.0)
Body mass index, kg/m^2	32.4±4.9
Caucasian, n (%)	38 (100)
Diabetes mellitus, n (%)	14 (36.8)
Dyslipidemia, n (%)	25 (65.7)
Coronary artery disease, n (%)	9 (23.6)
Medication use	
ACE inhibitor, n (%)	15 (39.5)
Angiotensin receptor blocker, n (%)	35 (92.1)
Direct renin inhibitor, n (%)	1 (2.6)
Diuretics, n (%)	38 (100)
Beta-blocker, n (%)	29 (76.3)
Alpha adrenergic blocker, n (%)	9 (23.6)
Calcium channel blocker, n (%)	35 (92.1)
Statin, n (%)	24 (63.2)

Abbreviation: ACE, angiotensin-converting enzyme.

Table 2 Baseline CT-derived measures at ablation and non-ablation zones within renal arteries

CT variables	Ablation zone[a] (n=38)	Non-ablation zone[a] (n=38)	*P*-value
Vessel volume (mm^3)	1,561.8±478.7	1,189.0±448.7	<0.001
Lumen volume (mm^3)	950.0±313.8	748.3±309.1	0.001
VWV (mm^3)	611.7±212.4	440.0±177.5	<0.001
P-VWV (%)	39.3±6.8	37.4±7.4	0.10

Note: [a]The ablation and non-ablation zones were defined as the segment before and after bifurcation of renal arteries, respectively.
Abbreviations: CT, computed tomography; P-VWV, percent vessel wall volume; VWV, vessel wall volume.

The averaged total length of analyzed renal arteries was 63.4±3.2 mm. Baseline CT-derived measures of ablation and non-ablation zones are shown in Table 2. Greater VWV (611.7±212.4 vs 440.0±177.5 mm^3, P<0.001) and P-VWV (39.3%±6.8% vs 37.4%±7.4%) were observed in the ablation zone, although the latter did not meet statistical significance (P=0.10). The ablation zone exhibited significantly larger vessel (1,561.8±478.7 vs 1,189.0±448.7 mm^3, P<0.001) and lumen (950.0±313.8 vs 748.3±309.1 mm^3, P=0.001) volumes. The distribution of P-VWV in each 5 mm segment of ablation and non-ablation zones is shown in Figure 2. The proximal segment of renal arteries was more likely to harbor larger amount of P-VWV (P=0.01 for overall; Figure 2).

Serial changes in vessel walls of renal arteries after the procedure

Changes in CT-derived measures of ablation and non-ablation zones are summarized in Table 3. On serial evaluation, greater progression of VWV (+106.3±87.4 vs +23.0±18.2 mm^3, P=0.001) and P-VWV (+6.7%±5.1% vs +3.6%±2.8%, P=0.001) was observed in the ablation zone. This segment was more likely to exhibit greater reduction in lumen volume (from −104.7±25.7 to −62.1±20.0 mm^3, P=0.03) accompanied with progression of P-VWV and VWV. There was no significant difference in regard to change in vessel volume between the segments (from −13.5±21.2 to −32.6±28.9 mm^3, P=0.52). Baseline VWV and P-VWV were negatively correlated to their changes (baseline VWV and change in VWV: r=−0.180, P=0.01; baseline P-VWV and change in P-VWV: r=^0.432, P=0.001). Figure 3 shows the cumulative frequency of P-VWV in ablation and non-ablation zones at baseline and 6 months after the procedure. Further detailed analysis of atheroma progression in each 5 mm segment is shown in Figure 4. More proximal segment of renal arteries was associated with greater progression of P-VWV (P=0.003 for overall; Figure 4).

Receiver-operating curve analysis was conducted to identify the optimal cutoff value of P-VWV in the ablation zone for predicting its substantial increase defined as change in P-VWV ≥10% (75 percentile of change in P-VWV), as shown in Figure 5. The optimal cutoff value of baseline P-VWV was 37.1%, and the area under the receiver-operating curve was 0.88. At this value, the sensitivity and specificity for predicting substantial change in P-VWV were 89.8% and 79.1%, respectively.

Observer variability

For the 20 renal arteries included in the analysis for intraobserver variability, there were a total of 1,127 images analyzed. The mean (SD) differences of vessel walls and lumen areas were 1.5 (0.7) and 0.8 (0.5) mm^2, respectively. Linear regression analysis showed close correlations between the original analysis and reanalysis (r=0.97 for the vessel area and r=0.98 for the lumen area). In regard to interobserver variability of the same 20 renal arteries, the mean (SD) differences were negligible for both vessel wall (1.8 mm^2 [1.0 mm^2]) and lumen (0.9 mm^2 [0.7 mm^2]) areas. Regression analysis showed close correlations between the original analysis and subsequent analysis (r=0.96 for the vessel area and r=0.97 for the lumen area).

Discussion

Despite a low frequency of renal artery stenosis following renal denervation procedure, serial changes in the vessel wall of renal arteries have not been characterized yet. The current serial volumetric CT analysis demonstrated greater increase in VWV in the ablation zone, particularly in areas more proximal and with significant preexisting atherosclerosis.

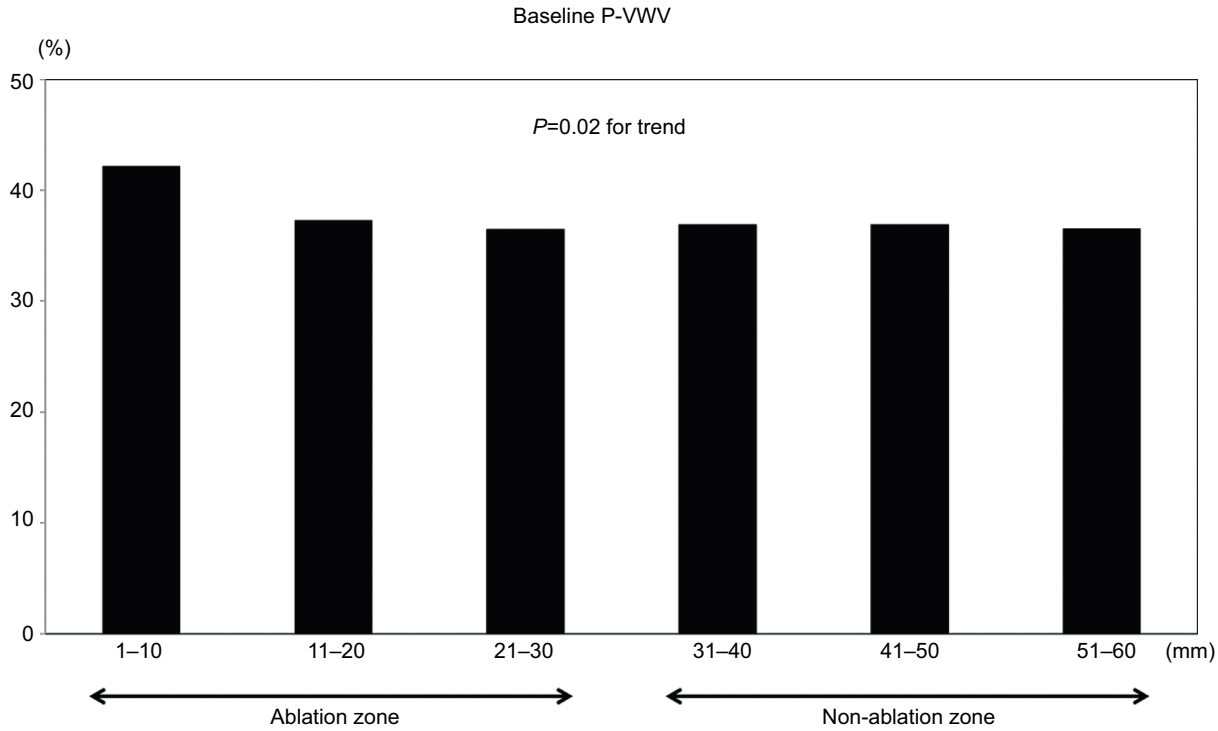

Figure 2 Baseline P-VWV in each 10 mm segment of renal artery.
Abbreviation: P-VWV, percent vessel wall volume.

Table 3 Serial changes in CT-derived measures at ablation and non-ablation zones within renal arteries

CT variables	Ablation zone (n=38)	Non-ablation zone (n=38)	*P*-value
Vessel volume (mm^3)	−13.5±21.2	−32.6±28.9	0.52
vs baseline	0.58	0.25	-
Lumen volume (mm^3)	−104.7±25.7	−62.1±20.0	0.03
vs baseline	0.001	0.001	-
VWV (mm^3)[a]	+106.3±87.4	+23.0±18.2	0.001
vs baseline	<0.001	0.001	-
P-VWV (%)[a]	+6.7±5.1	+3.6±2.8	0.001
vs baseline	<0.001	<0.001	-

Note: [a]Adjusted for baseline values.
Abbreviations: CT, computed tomography, P-VWV, percent vessel wall volume VWV, vessel wall volume.

This finding suggests the potential association of catheter-based renal sympathetic denervation with vascular thickening in the ablation area.

A recent study using intravascular optical coherence tomography reported the occurrence of endothelial–intimal edema and thrombus formation after renal sympathetic denervation using the Symplicity™ or EnligHTN catheter.[15] Also, a significant reduction in luminal diameter of renal artery was observed.[15] These findings suggest local vascular injury induced by ablation systems in vivo. However, due to the absence of follow-up studies, it has not been elucidated whether these vascular damages contribute to the progression of renal atherosclerosis following the procedure. Furthermore, since the shallow penetration depth of optical coherence tomography imaging is not suitable for evaluating atheroma volume, it has not yet been fully characterized to assess the effects of renal denervation on atheroma burden within renal arteries. In the current study, serial volumetric CT analysis demonstrated atheroma progression in the ablation zone. Another observation has reported pulmonary vein stenosis after radiofrequency ablation in patients with atrial fibrillation.[16,17] Mechanistically, extensive fibrosis, neointimal hyperplasia, and a marked inflammatory process have been reported to occur after radiofrequency or ultrasound energy delivery in canine models.[18] These mechanisms might potentially induce the progressive changes of intimal thickening within renal arteries after renal sympathetic denervation procedure. Whether these vascular changes influence blood pressure and kidney function after renal denervation is not yet evaluated. Mechanistically, renal artery narrowing could reduce blood flow and activate the renin–angiotensin–aldosterone system, thereby elevating blood pressure and

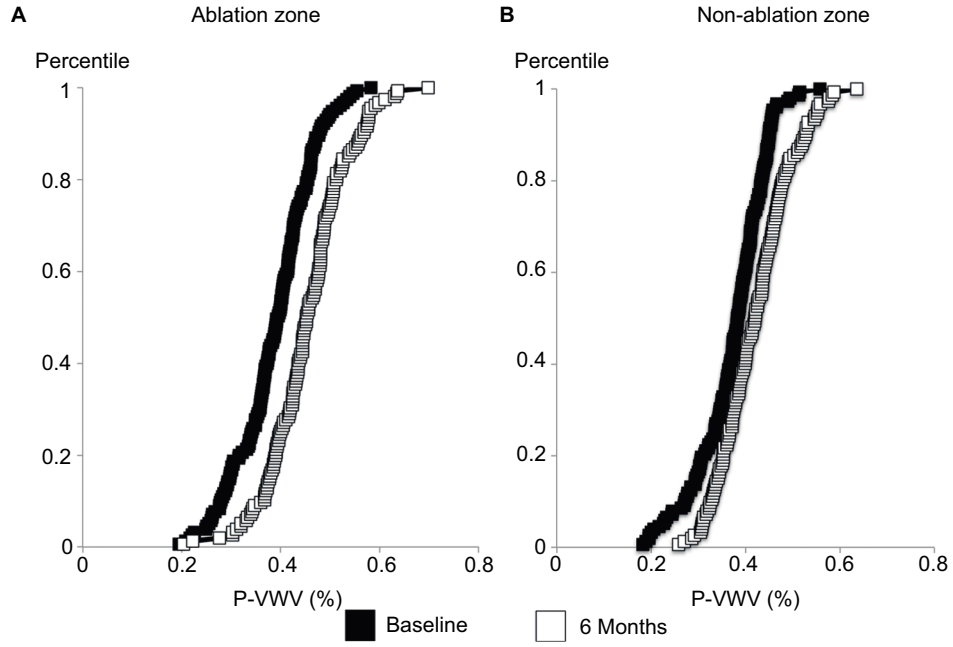

Figure 3 Cumulative distribution curve for baseline and 6-month P-VWV at the ablation and non-ablation zones.
Notes: (**A**) The ablation zone; (**B**) the non-ablation zone.
Abbreviation: P-VWV, percent vessel wall volume.

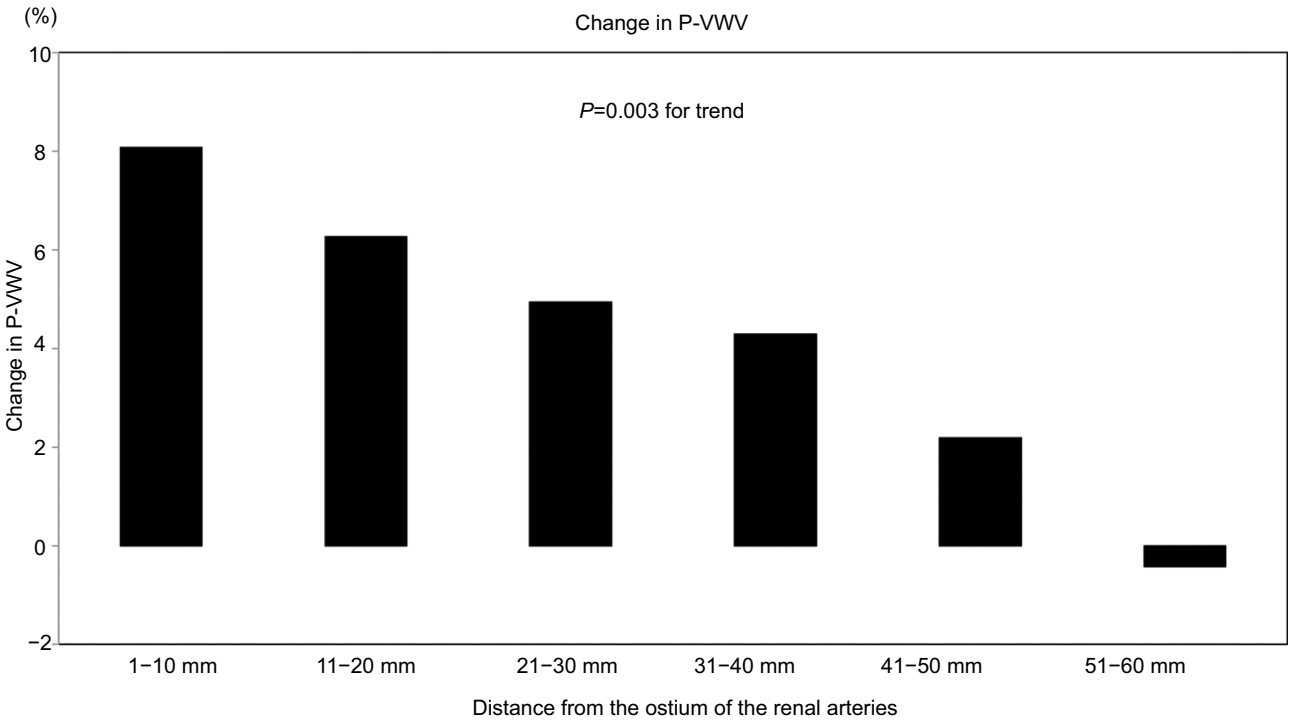

Figure 4 Change in P-VWV in each 10 mm segment of the renal artery.
Abbreviation: P-VWV, percent vessel wall volume.

deteriorating renal function; however, this is mere postulation and these potential effects require further investigation.

In the current study, change in CT-derived measures of vessel walls was predominantly observed at more proximal segments of the renal arteries compared to the distal segments. The majority of published case reports also showed that renal artery stenosis post-procedure was more prominent in the proximal segments of the renal arteries.[10–12,19] We noted

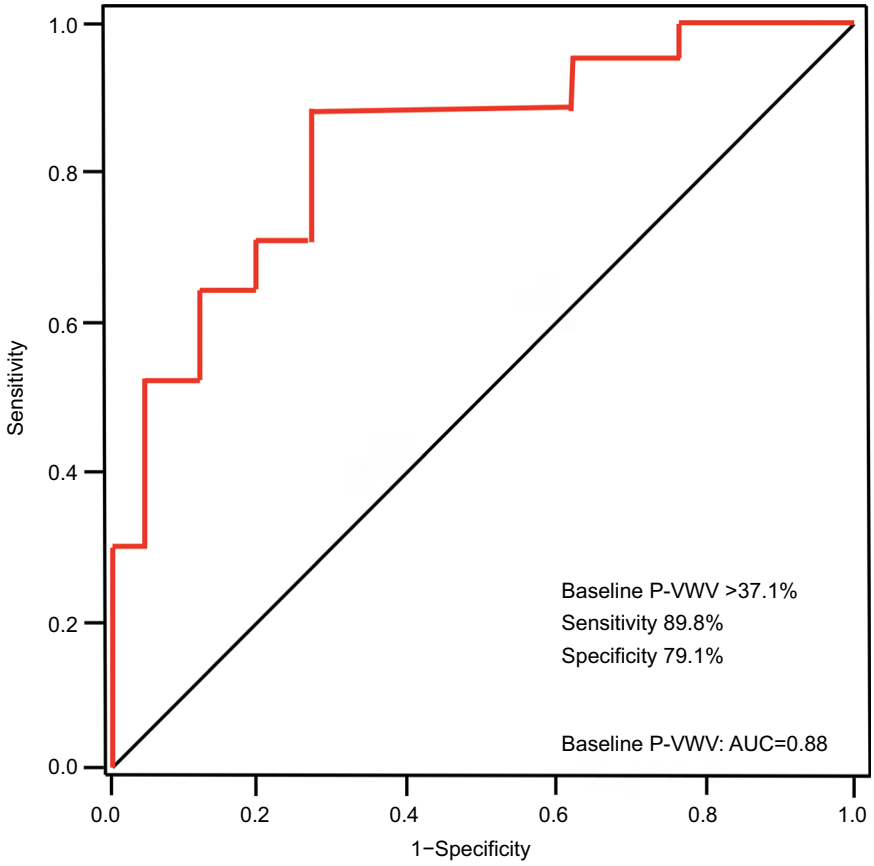

Figure 5 ROC analysis of CT-derived P-VWV for predicting its substantial increase in the ablation zone.
Note: ROC curves for P-VWV in the ablation zone of the renal artery.
Abbreviations: AUC, area under the curve; CT, computed tomography; P-VWV, percent vessel wall volume, ROC, receiver-operator characteristic.

that the most proximal 10 mm segment had the greatest baseline atheroma volume. Delivery of energy too close to a diseased vessel wall might be responsible for exaggerated tissue response causing more vascular damage at the proximal segment of renal arteries.

The EnligHTN I study did not enroll patients having apparent lesions on CT renal angiography.[13] However, over 80% of the study subjects exhibited baseline P-VWV >30% in the entire artery. This finding indicates the presence of extensive mild renal atherosclerosis in resistant hypertensive patients. Since patients with resistant hypertension are more likely to have risk factors in addition to uncontrolled blood pressure levels, these atherogenic backgrounds potentially contribute to harboring distinct atheroma burden in renal arteries.

To date, no study has conducted serial volumetric CT analysis of renal arteries. We sought to acquire cross-sectional CT images of the whole renal artery at 1 mm interval. This analytic method enables the measurement of plaque area in each image by tracing the luminal and outer wall boundaries, as previously employed with intravascular ultrasound imaging of coronary atherosclerosis.[20] The current CT measurement approach is highly reproducible. In addition, since any effective approach to predict the risk of renal artery stenosis has not been established yet, evaluating renal arteries with CT imaging is possible and might be useful to estimate the risk of renal artery damages after the procedure.

A number of study limitations should be noted. First, the patient population was relatively small, and only one type of catheter was used for all subjects and it remains unknown whether the changes are mirrored with other devices. The current study does not have a sham group who do not receive the procedure, and therefore, comparisons of serial change in segments before the first bifurcation between the sham group and patients receiving renal denervation therapy cannot be performed. While the current study investigated the association of renal nerve ablation with progression, it did not evaluate other factors causing renal vessel damage, such as injury from guiding catheter at the very proximal of renal artery.

Conclusion

In summary, serial CT imaging of renal arteries elucidated a greater increase in VWV of renal arteries receiving sympathetic denervation with the EnligHTN catheter used in this study. The current study indicates that the extent of atheroma burden within renal arteries could be a predictor of elevated risk of vascular damages after renal sympathetic denervation.

Acknowledgments

We thank the following St Jude Medical personnel: Yan Zheng for statistical analyses and Anne Marie Harcarik RN and Steven Madej BS for help in preparing the manuscript.

EnligHTN I trial was funded by St. Jude Medical Inc., St Paul, MN, USA.

Disclosure

The authors report no conflicts of interest in this work.

References

1. Papademetriou V, Rashidi AA, Tsioufis C, Doumas M. Renal nerve ablation for resistant hypertension: how did we get here, present status, and future directions. *Circulation*. 2014;129(13):1440–1451.
2. Böhm M, Linz D, Ukena C, Esler M, Mahfoud F. Renal denervation for the treatment of cardiovascular high risk-hypertension or beyond? *Circ Res*. 2014;115(3):400–409.
3. Böhm M, Linz D, Urban D, Mahfoud F, Ukena C. Renal sympathetic denervation: applications in hypertension and beyond. *Nat Rev Cardiol*. 2013;10(8):465–476.
4. Krum H, Schlaich M, Whitbourn R, et al. Catheter-based renal sympathetic denervation for resistant hypertension: a multicentre safety and proof-of-principle cohort study. *Lancet*. 2009;373(9671):1275–1281.
5. Symplicity HTN-2 Investigators, Esler MD, Krum H, Sobotka PA, Schlaich MP, Schmieder RE, Böhm M. Renal sympathetic denervation in patients with treatment-resistant hypertension (The Symplicity HTN-2 Trial): a randomised controlled trial. *Lancet*. 2010;376:1903–1909.
6. Kaiser L, Beister T, Wiese A, et al. Results of the ALSTER BP real-world registry on renal denervation employing the Symplicity system. *EuroIntervention*. 2014;10(1):157–165.
7. Bhatt DL, Kandzari DE, O'Neill WW, et al. SYMPLICITY HTN-3 Investigators. A controlled trial of renal denervation for resistant hypertension. *N Engl J Med*. 2014;370:1393–1401.
8. Townsend RR, Mahfoud F, Kandzari DE, et al. SPYRAL HTN-OFF MED trial investigators. Catheter-based renal denervation in patients with uncontrolled hypertension in the absence of antihypertensive medications (SPYRAL HTN-OFF MED): a randomised, sham-controlled, proof-of-concept trial. *Lancet*. 2017;390(10108):2160–2170.
9. Steigerwald K, Titova A, Malle C, et al. Morphological assessment of renal arteries after radiofrequency catheter-based sympathetic denervation in a porcine model. *J Hypertens*. 2012;30(11):2230–2239.
10. Kaltenbach B, Id D, Franke JC, et al. Renal artery stenosis after renal sympathetic denervation. *J Am Coll Cardiol*. 2012;60(25):2694–2695.
11. Vonend O, Antoch G, Rump LC, Blondin D. Secondary rise in blood pressure after renal denervation. *Lancet*. 2012;380(9843):778.
12. Worthley SG, Tsioufis CP, Papademetriou V. Regarding "Severe bilateral renal artery stenosis after transluminal radiofrequency ablation of renal sympathetic nerve plexus". *J Vasc Surg*. 2015;62(2):539.
13. Worthley SG, Tsioufis CP, Worthley MI, et al. Safety and efficacy of a multi-electrode renal sympathetic denervation system in resistant hypertension: the EnligHTN I trial. *Eur Heart J*. 2013;34(28):2132–2140.
14. Kataoka Y, Puri R, Pisaniello AD, et al. Aortic atheroma burden predicts acute cerebrovascular events after transcatheter aortic valve implantation: insights from volumetric multislice computed tomography analysis. *EuroIntervention*. 2016;12(6):783–789.
15. Templin C, Jaguszewski M, Ghadri JR, et al. Vascular lesions induced by renal nerve ablation as assessed by optical coherence tomography: pre- and post-procedural comparison with the Simplicity catheter system and the EnligHTN multi-electrode renal denervation catheter. *Eur Heart J*. 2013;34(28):2141–2148.
16. Robbins IM, Colvin EV, Doyle TP, et al. Pulmonary vein stenosis after catheter ablation of atrial fibrillation. *Circulation*. 1998;98(17):1769–1775.
17. Packer DL, Keelan P, Munger TM, et al. Clinical presentation, investigation, and management of pulmonary vein stenosis complicating ablation for atrial fibrillation. *Circulation*. 2005;111(5):546–554.
18. Taylor GW, Kay GN, Zheng X, Bishop S, Ideker RE. Pathological effects of extensive radiofrequency energy applications in the pulmonary veins in dogs. *Circulation*. 2000;101(14):1736–1742.
19. Jaén Águila F, Mediavilla García JD, Molina Navarro E, Vargas Hitos JA, Fernández-Torres C. Bilateral renal artery stenosis after renal denervation. *Hypertension*. 2014;63(5):e126–e127.
20. Nicholls SJ, Tuzcu EM, Sipahi I, Schoenhagen P, Nissen SE. Intravascular ultrasound in cardiovascular medicine. *Circulation*. 2006;114(4):e55–e59.